Noname manuscript No.
(will be inserted by the editor)

Counterion condensation, ion pairing and scattering properties of carboxymethyl cellulose with mono- and di-valent ions

Elmira Abbasi GharehTapeh · Takaichi Watanabe · Ferenc Horkay · Can Hou · Carlos G. Lopez · Max Hohenschutz

Received: date / Accepted: date

Elmira Abbasi GharehTapeh
Materials Science and Engineering Department, The Pennsylvania State University,
80 Pollock Rd, State College, PA 16802, USA

Takaichi Watanabe
Department of Applied Chemistry, Graduate School of Environmental, Life, Natural Science, and Technology,
Okayama University, 3-1-1 Tsushima-naka, Kita-ku, Okayama 700-8530, Japan

Ferenc Horkay
Section on Quantitative Imaging and Tissue Sciences, Eunice Kennedy Shriver National Institute of Child Health and Human Development,
National Institutes of Health, Bethesda, MD 20892, USA

Can Hou
Institute of Physical Chemistry, RWTH Aachen University,
Landoltweg 2, 52074 Aachen, Germany

Carlos G. Lopez
Materials Science and Engineering Department, The Pennsylvania State University,
80 Pollock Rd, State College, PA 16802, USA
E-mail: cvg5719@psu.edu

Max Hohenschutz
Institute of Physical Chemistry, RWTH Aachen University,
Landoltweg 2, 52074 Aachen, Germany
E-mail: hohenschutz@pc.rwth.de

Abstract We study the scattering and conductometric properties of a semiflexible polyelectrolyte, carboxymethyl cellulose (CMC), with monovalent and divalent counterions in aqueous media without added salt. The scattering patterns for the magnesium salts of CMC display a broad shoulder instead of the scattering peak observed for the monovalent salts. This suggests weaker electrostatic repulsion between chains and a consequent loss of local order. The result is consistent with conductivity measurements, which reveal that the effective charge of the backbone for MgCMC is approximately half that of NaCMC. The decrease in charge density agrees with Oosawa-Manning condensation, which expects the charge density to be inversely proportional to the counterion valence. Alkali metal counterions show large differences in ion-pair formation but only a weak effect in counterion condensation. We suggest that paired ions are a subset of condensed ions. A review of different methods to evaluate counterion condensation, including potentiometry, osmometry and viscosity-based methods is presented. Qualitative agreement between these methods is found and possible reasons for the discrepancies are discussed.

Keywords Polyelectrolyte · Counterion Condensation · Carboxymethyl cellulose · SAXS · Conductivity · Ion pairing

Introduction

Ion-polymer interactions play a central role in a variety of systems, for example in biological processes.(Tasaki, 2012; Verdugo, 2005; Sircar et al., 2013; Wnek, 2016) The role of ions is complex: they stabilize the local structures, and ion binding can also affect the intrinsic properties of the polymer molecules, such as flexibility, electrostatic interactions and the overall thermodynamics of the system. Due to long range electrostatic interaction, the physical picture of low salt polyelectrolyte solutions is still not well understood.(Buvalaia et al., 2023; Slim et al., 2022; Zhou et al., 2024) To account for the effects of concentration for polyelectrolyte solution in the semidilute and concentrated regimes where most of the experimental studies are performed, the scaling approach has been used to model the behavior of polyelectrolyte solutions.(Dobrynin and Rubinstein, 2005; Liao et al., 2007; Carrillo and Dobrynin, 2011; Gulati et al., 2023; Lopez et al., 2024) It has been demonstrated that in many systems, especially in the vicinity of ion-induced phase transition, the physical response is governed by universal scaling principles. Various physical forces and interactions are implicated in these processes, including electrostatic repulsion and attraction, hydrophobic and hydrophilic interactions, hydrogen bonding and van der Waals forces. (Hirotsu, 1994; Mussel et al., 2021)

Polyelectrolytes are used in different fields such as foods, water treatment and oil recovery. The molecular origin of the unique behavior of polyelectrolytes, which is also a fundamental problem related to many biological processes such as protein folding, DNA condensation and origin of life is still poorly understood.(Pineda et al., 2024; Agrawal et al., 2024) The properties of charged polymers are influenced the intrinsic properties of the chains (e.g., backbone rigidity), molecular mass, the concentration and valence of counterions, as well as inter- and intramolecular interactions (e.g., ion condensation, hydration, hydrogen bonding). To date, no satisfactory theoretical framework embodying the relationship between molecular/supramolecular structure, macroscopic properties and biological function of synthetic or natural polyelectrolyte molecules has been developed.

Condensation and binding

Two concepts are commonly used to describe polyion-counterion interactions. The first is counterion condensation, which refers to the accumulation of counterions in the vicinity of the backbone due to electrostatic attraction from the polyion. The condensed counterions do not contribute to the osmotic pressure of the solution or to transport properties such as electrical conductivity. The second concept is ion-pairing, which occurs when the counterion comes in close contact with the ionic group of the polyelectrolyte. What qualifies as a close contact is difficult to demarcate, and different ideas have been put forward.(Marcus and Hefter, 2006; Gregory et al., 2022) The solvent in the close vicinity of an ion experiences a huge pressure from the electrostatic field and as a result its density increases, a phenomenon known as electrostriction.(Hemmes, 1972) When an ion-pair forms, some of the electrostricted solvent is released, leading to a volume increase. This provides a functional definition for ion-pair formation.

Understanding counterion condensation is important because virtually all solution properties are influenced by the effective charge of the chain. Ion-pairing does not influence many macroscopic solution properties, but it plays a crucial role in applications such as ion-recovery processes.

Oosawa-Manning condensation

When a polyelectrolyte dissolves in a solvent, a fraction of the counterions dissociate from the backbone and the rest stay in the close vicinity of the chain's backbone, thereby lowering the effective polyion charge.(Essafi et al., 1999; Matsumoto et al., 2022; Tang and Rubinstein, 2022; Muthukumar, 2004) The first successful attempt to describe this phenomena, known as counterion condensation was the theory of Oosawa and Manning.(Manning, 1969; Oosawa, 1971) In their model, an infinite, isolated rod-like polyelectrolyte is considered. Counterions are treated as point-like charges interacting via Debye-Hückel screened potentials and the backbone as possessing a uniform charge density. Under these (and other) assumptions, the famous result is obtained that monovalent counterions will condense onto the backbone until the effective charge is reduced to one charge per Bjerrum length (l_B), with:

$$l_B = \frac{e^2}{k_B T 4\pi\varepsilon}$$

where e is the electrostatic unit of charge, ε the dielectric constant, k_B is Boltzmann's constant and T the absolute temperature.

The critical charge on the chain is predicted to be:

$$\mu_{eff} = \frac{e}{z l_B}$$

where z is the valence of the counterion. This means that when the bare charge of a chain (the charge of the backbone without counterions) exceeds μ_{eff}, counterions will bind or condense onto the chain until the effective charge of the chain (i.e. the sum of the charge of the backbone and the neutralising counterions) decreases to a $e/(l_B z)$, that is one charge per Bjerrum length for monovalent counterions and one charge per two Bjerrum lengths for divalent counterions. For higher-valent counterions, specific ion effects are strong, and treatments based on Debye-Hückel screening are not appropriate.(Lopez et al., 2024; Ehtiati et al., 2022; Smiatek, 2020)

Counterion condensation is often discussed in terms of the coupling parameter (u), which is the ratio between the Bjerrum length and d, the distance between ionic groups along the backbone ($u = l_B/d$). The Manning model predicts counterion condensation to set in when u exceeds a value of 1 for monovalent ions or 2 for divalent ones. A useful way of experimentally quantifying counterion condensation is to measure their activity using ion-selective electrode potentiometry. The theory of Manning predicts for the activity coefficient of polyelectrolytes with monovalent counter-ions in salt-free solution:

$$\Gamma = \begin{cases} e^{-u/2} & \text{if } u < 1 \\ \frac{1}{\sqrt{eu}} & \text{if } u > 1 \end{cases} \tag{1}$$

and for divalent counterions:(Manning, 1974)

$$\Gamma = \begin{cases} e^{-u} & \text{if } u < \frac{1}{2} \\ \frac{1}{2\sqrt{eu}} & \text{if } u > \frac{1}{2} \end{cases} \tag{2}$$

Note that according to Eqs. 1 and 2, the activity of the free counterions is lower than their concentration.

The Oosawa and Manning models are derived for rigid and isolated chains (i.e. rod-like polyelectrolytes at infinite dilution). Its extension to higher concentrations results in more complex behaviour.(O'Shaughnessy and Yang, 2005; Oosawa, 1971) Experimental evidence on flexible polyelectrolytes (Wandrey, 1999; Wandrey et al., 2000) show that below the overlap concentration counterion dissociation increases upon dilution, approaching the no condensation limit at infinite dilution, in agreement with later simulation results (Liao et al., 2003) and contradicting the Oosawa-Manning model. Interestingly, the OM model appears to hold in the semidilute regime.

A complication that arises when applying the Oosawa-Manning model to flexible or semiflexible polyelectrolytes because, unlike for the case of rigid chains, the conformation of the chain may depend on the effective charge of the backbone, thus requiring a more involved calculation where the free energy of the chain and the counterions are calculated self-consistently.(Muthukumar, 2004) Further, interactions between counterions and polymers include effects arising from sharing of hydration shells and ion-pair formation, not accounted for in the Oosawa-Manning theory. (Lytle et al., 2021; Marcus and Hefter, 2006)

The effective charge of the polyelectrolyte backbone influences many solution properties, including the charge transport, (Diederichsen et al., 2019; Kondou et al., 2023; Marioni et al., 2024) osmotic pressure, (Colby, 2010) and phase behaviour.(Lopez et al., 2024; Chen et al., 2021) Therefore, it is of interest to understand how counterion condensation depends on experimental variables. Here we investigate how the properties of the counterion influence the degree of condensation for semiflexible polyelectrolyte carboxymethyl cellulose (CMC), an extensively studied anionic cellulose ether. (Lopez et al., 2015, 2018; Jimenez et al., 2020; Różańska et al., 2019; Behra et al., 2019; Jimenez et al., 2022; Arumughan et al., 2023; Wagner et al., 2023; Legrand et al., 2024; Yoshida et al., 2024) NaCMC finds many applications as a thickener, moisture retainer and structuring agent in pharmaceutical, food, wine, cosmetic and other formulations.(Kim et al., 2022; Wang et al., 2024; Liu and Zhao, 2019; Hou et al., 2024b; Kong et al., 2024; Zhang et al., 2022, 2024; Cai et al., 2025; Sommer, 2025)

Divalent cations play a key role in many biopolymer systems. In general, experiments to determine the interactions between ions and biopolymers are difficult to perform, because above a relatively low ion concentration multivalent cations cause phase separation or gelation of the charged macromolecules.(Sharratt et al., 2020, 2021) We study the structure and

transport properties of carboxymethyl celluloses with varying degrees of substitution (DS), and quantify the effects of monovalent and divalent counterions on their physical properties. While carboxymethyl cellulose is normally employed as a sodium salt, formulations containing NaCMC often contain divalent ions or come in contact with them when they are diluted with tap water. The interaction of divalent ions with polyelectrolytes is more complex than that of monovalent ions due to ion-specific effects.(Horkay and Douglas, 2025; Lopez et al., 2024; Mussel et al., 2019; Beyer and Holm, 2024; Chang and Yethiraj, 2003; Glisman et al., 2024) Here we focus on the Mg^{2+} ion, which displays weak specific-ion interactions with carboxylate groups of CMC.(Sharratt et al., 2020)

Activity of CMC counterions

Literature results for the activity coefficient of NaCMC and MgCMC are compiled in Fig. 1. All data were obtained using ion-selective potentiometry. The theory of Manning (Eqs. 1 and 2), shown as lines, under-predicts the activity coefficient for both monovalent and divalent salts of CMC over the entire charge density range studied.

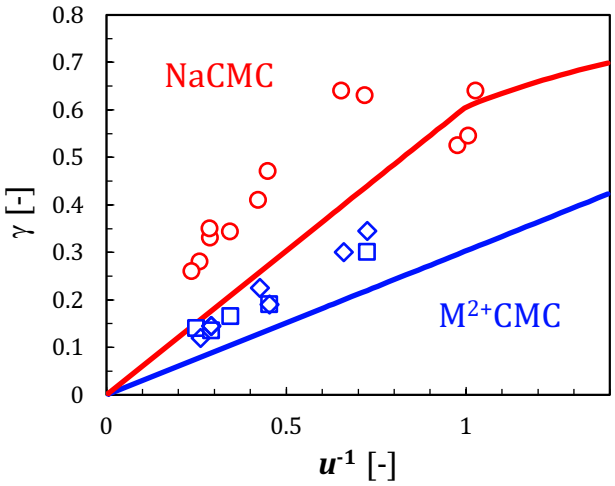

Fig. 1 Counterion activity of carboxymethyl celluloses with different degrees of substitution as a function of the charge coupling parameter. Lines are predictions of the Manning model. Data are from refs. (Rinaudo and Loiseleur, 1973; Rinaudo et al., 1971; Rinaudo and Milas, 1974; Rinaudo and Mils, 1978; Rinaudo, 1973; Rinaudo and Milas, 1975; Nagasawa and Kagawa, 1957). Red points are for NaCMC and blue points are for MgCMC (squares) or CaCMC (diamonds).

In interpreting the data in Fig. 1 it should be noted that the distribution of substituents along the CMC backbone is not homogeneous. The degree of heterogeneity depends on the synthesis procedure used. For reference, the data of Kono et al(Kono et al., 2016b,a) for NaCMC synthesised via the slurry process show that for DS $= 0.7$, or equivalently $u \simeq 1$, corresponding to the lowest charge density in Fig. 1, there exist $\simeq 5\%$ of monomers with two carboxymethyl groups and an equal percentage with three substituted groups. Such substitution patterns are expected to display greater condensation than homogeneous ones because regions with high substitution coexist with regions of low substitution. For very high

DS, where the average charge spacing is much lower than l_B, heterogeneity in substitution is not important because having two adjacent charges separated by more than l_B becomes highly improbable. For such samples, Manning's theory is expected to work best. In fact, Fig. 1 shows the opposite result, with the Manning prediction agreeing with low substitution samples but underpredicting the activity of the highly substituted ones. We conclude that the agreement for low DS (high u^{-1}) samples is likely accidental.

Ion specificity and counterion binding

Beyond charge condensation, the size, electronic structure and hydration of an ion make the binding to an oppositely charged group ion-specific. For monovalent ions, such as Li^+, Na^+ or Cs^+, binding correlates with the size of the ion according to Collin's concept of matching water affinities. (Vlachy et al., 2009; Collins, 2004) According to Collins concept, at small and strongly hydrated carboxylate groups such as in CMC, small ions, such as Li^+, are expected to bind most strongly due to a match of hydration water in contrast to large Cs^+, which should bind less strongly due to a hydration mismatch.

Evidence for the Collin's concept is found for the alkaline metal salts of CMC in the ultrasound absorption studies of Milas and co-workers: When a counterion forms an ion-pair with the side group on the polymer, electrostricted water is released, leading to a change in volume.(Tondre and Zana, 1971, 1972; Zana and Tondre, 1975b; Zana, 1975; Zana and Tondre, 1975a; Koda et al., 2004) Ultrasound absorption is sensitive to processes which generate volume changes and thus can be used to track the strength of ion-pair formation in polyelectrolyte solutions. Counterion condensation does not usually involve a volume change and therefore does not show up in ultrasound absorption spectra, see (Komiyama et al., 1974, 1976; Tondre and Zana, 1975; Tondre et al., 1978) Fig. 2a plots the excess ultrasound absorption of HCMC (DS = 2.49) solutions with respect to water ($\delta\psi$) as a function of degree of neutralisation with various hydroxides. The black arrow marks $i = 0.26$, corresponding to $u \simeq 1$, the onset of Oosawa-Manning condensation. For $i \lesssim 0.26$, $\delta\omega$ is independent of degree of neutralisation and counterion type, as expected because below the condensation threshold, no site-binding occurs. At higher degrees of neutralisation, the smaller counterions give rise to higher ultrasound absorption, indicating stronger ion-pair formation. Owing to its large size, it is often assumed that TMA^+ does not site-bind to the CMC backbone. Further assuming that replacing sodium by tetramethyl ammonium counterions does not change the viscoelastic relaxations of the CMC solutions, the difference in ultrasound absorption between NaCMC and TMACMC solutions ($\Delta\Psi_{TMA}$) can be used as a direct measure of site-binding strength. $\Delta\Psi_{TMA}$ is plotted as a function of DS multiplied by the degree of ionisation (i) in Fig. 2b, where it is observed that data follow a linear relationship which intercepts the abscissa at iDS$\simeq 0.67$, corresponding to $u \simeq 1$. These data provide evidence that site-binding via ion-pair formation does not take place in the absence of counterion condensation.

For divalent ions, the Collins concept breaks down, as the electronic structure of the divalent cation allows for complexation and chelation with an ionic ligand, such as carboxylate. The Irving-Williams series describes the differences in relative stability of aqua complexes for divalent transition metal ions. For divalent cations, the ease of removing an aqua ligand is considered the main factor, while the properties of the ionic ligand, such as carboxylate, surprisingly don't play a role. Experimental results on the strength of binding of divalent metal ions to partially neutralised CMC by Rinaudo and Milas(Rinaudo and Milas, 1974) display different trends than expected from the Irving-Williams series. Both the

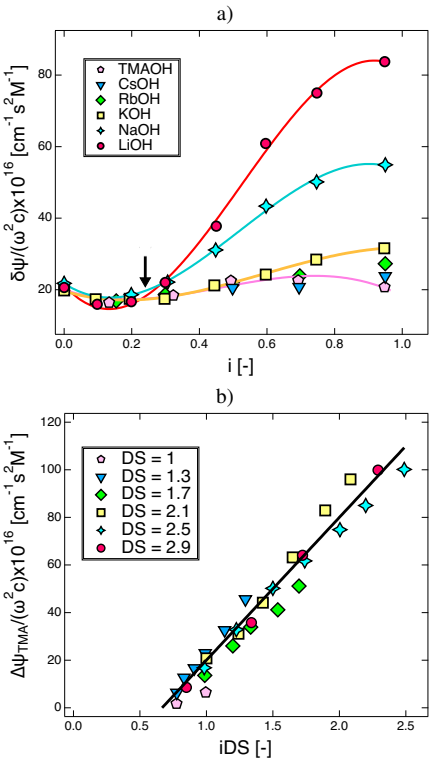

Fig. 2 Ultrasound absorption properties of CMC polymers. a: excess ultrasound absorption with respect to water at a frequency of $\omega = 5.04$ MHz for HCMC with DS = 2.49 and $c = 0.1$ M neutralised to different degrees with TMA or alkaline metal hydroxides. The black arrow indicates the point at which the distance between ionised groups is equal to the Bjerrum length ($u \simeq 1$). Lines are guides to the eye. b: difference in ultrasound absorption of HCMC neutralised with NaOH with respect to the same polymer neutralised with TMAOH ($\omega = 2.8$ MHz). The DS of the various polymers are indicated on the legend. Line is a guide to the eye. Data are from (Milas, 1974; Zana et al., 1971).

Collin's concept and the Irving-Williams series are useful tools to understand ion-specific binding. However, deviations from them are commonly observed.(Kherb et al., 2012)

Influence of ion type and valence on chain conformation

Studies on the influence of ion type on the thermodynamics of ion binding to polyelectrolytes are abundant. The influence of ion type on solution structure has received less attention.(Dubois and Boué, 2001; Combet et al., 2005, 2011; Hotton et al., 2023; Chremos and Douglas, 2018, 2017, 2016) With some exceptions,(Hotton et al., 2024) the nature of counterion type for monovalent ions is found to have a small influence on the structural (Kaji et al., 1984; Zhang et al., 2001) and dynamic (Lopez and Richtering, 2019; Lopez et al., 2021) parameters of solutions. For example, the overlap concentration of CMCs with different divalent ions and of PSS with sodium and tetra-alkyl-ammonium ions were found to be insensitive to ion type, indicating that the dilute chain size remains unchanged.(Lopez and Richtering, 2019; Gulati et al., 2024) Kaji reports a weak dependence of the correla-

tion length of PSS solutions with H^+ and alkaline metal counterions.(Kaji et al., 1984) The weak influence of counterion type (for a fixed counterion valence) on conformation and dynamics contrasts with large differences observed for the binding constants in equilibrium dialysis.(Hen and Strauss, 1974) This suggests that competitive binding of ions is influenced by site-binding strength. On the other hand, counterion condensation, which dictates the effective charge of the backbone and thereby the conformational and dynamic properties of chains may be largely insensitive to site-binding strength.

Based on the above discussion we hypothesize that Oosawa-Manning theory holds for CMC with various counterions and that ion-specific effects should not have a strong influence on counterion condensation.

Materials and Methods

CMC polymers: Sodium salts of CMC were purchased from Sigma Aldrich (S1-S7) or donated (S8-S10) by KelcoCP or Dow. Several of these samples were characterised in previous studies, as noted in table 1. The degree of substitution was determined (either in this study or in our prior works) by back titration of HCMC, where the acid is prepared by dialysis as described in ref. (Lopez and Richtering, 2019), and not by alcohol wash method because the latter can yield artificially low DS values for highly substituted samples.(Hedlund and Germgård, 2007) The exception was S5, for which the DS value from the certificate of analysis provided by Sigma-Aldrich was used. Sodium salts were purified by dialysis against DI water until the conductivity of the bath reached a stable value of 2-3 μS/cm after at least 6 hrs of dialysis. The magnesium salts were prepared by addition of $\times 20$ molar excess $MgCl_2$ to a CMC solution followed by extensive dialysis against DI water. Alkaline metal salts of CMC were prepared by neutralising dry HCMC with the corresponding hydroxyde to pH > 12 followed by dialysis against DI water. All samples were freeze dried after dialysis. The molecular weights of polymers S1-S5 were evaluated in earlier work, from static light scattering or intrinsic viscosity measurements, see Table 1.

Table 1 Sample properties for different polymers used. The molar mass of an average repeating unit is 160+80×DS for sodium salts and 160+69×DS for magnesium salts. [a] value obtained from manufacturer's certificate of analysis.

Polymer	DS	Notes
S1	1.3	Sample 240k in (Lopez, 2020), see also (Lopez and Richtering, 2019).
S2	0.97	Same as polymer in (Hou et al., 2025), conductivity and SAXS data reported in (Hou et al., 2025).
S3	0.72	Same as polymer in (Lopez and Richtering, 2021)
S4	0.73	Sample CMC85k in (Lopez, 2020), DS was evaluated for this study.
S5	0.81	Sample CMC94k in (Lopez, 2020)
S6	0.78[a]	
S7	1.4	
S8	0.87	WALOCEL-CRT 15000 PPA , donated by Dow
S9	0.79	Cekol-2000A, donated by CP Kelco
S10	0.92	Cekol-30000A, donated by CP Kelco

Electrical Conductivity: Two setups were used: One setup is the same as that described in (Hou et al., 2025), whereby a SevenMulti Dual pH/conductivity meter (Mettler Toledo) was used, with the probe inserted into a 10 mL centrifuge vial containing roughly 3 mL of the sample solution, which was placed in a temperature-controlled water bath and kept at 25 °C. The second setup used a SevenExcellence pH/conductivity meter (Mettler Toledo). InLab 741 conductivity probe with 2 steel poles with an integrated temperature sensor were used to measure the conductivity over the 0.001- 500 μS/cm range. InLab710 conductivity cell with 4 platinum poles were also used, measuring the conductivity through the range of 0.01-500 mS/cm. Samples in the conductivity overlap range (100-500 μS/cm) were measured by both probes to confirm the consistency of the results. The InLab 741 probe was calibrated using 100 μS/cm standard solution placed inside a water bath to equilibrate to 25°C. Tbe InLab710 conductivity cell was calibrated in the same manner using 1413 μS/cm standard solution.

Small Angle X-ray Scattering (SAXS): SAXS experiments were carried out at an in-house instrument and at the Spring-8 synchrotron facility in Hyogo, Japan (Beamline BL40). The instrument configurations and measurement procedures were the same as described in previous publications (Hou et al., 2025; Gulati et al., 2024). In-house SAXS-measurements were performed at room temperature on a Nanoinxider instrument from Xenocs. The copper source (λ =0.154 Å) with simultaneous small-angle and wide-angle detection enabled to access a q−range of 0.1-40 nm^{-1}. Scattered intensities were scaled to absolute scale by standard-less absolute intensity calibration. Borosilicate capillaries from WJM glass were used as sample containers.

Small Angle Neutron Scattering (SANS): Neutron scattering experiments were carried out at the SANS30G beamline of the NIST research reactor ($0.0034 < q/\text{Å}^{-1} < 0.4$) and the D11 beamline of the ILL, Grenoble, ($0.0022 < q/\text{Å}^{-1} < 0.45$). Samples were loaded into quartz cuvette and data were reduced into absolute units using the standard procedure provided by the facility.

Thermogravimetric analysis (TGA): Thermogravimetric analysis was carried out with a Discovery TGA 550 with a nitrogen flow of 50 mL/min. Relatively small masses of CMC samples (6 ± 2 mg) were loaded onto clean, tared 100 μL platinum TGA pans without lids. The samples were heated to 120 °C and held for one hour and were then heated from 120 to 420 °C at a rate of 10 °C/min. The water content fo the CMC was evaluated from the mass loss at the first stage (25-120 °C).

Measurements were performed at $T = 25$ °C unless otherwise indicated. Scattering and conductivity data are tabulated in the supporting information.

Results and Discussion

Small angle scattering

SAXS curves for MgCMC were measured for samples S1-S4 and S6-S10. For the NaCMC salts, we measured S7 over a concentration range of 2-40 g/L. SAXS data for the sodium salts of samples S1 and S2 were reported in earlier studies(Gulati et al., 2024; Hou et al., 2024a; Sharratt et al., 2020). SANS data for sample S1 was reported in (Gulati et al., 2024; Sharratt et al., 2020) and additional measurements for the same polymer in the sodium and magnesium forms are reported here. We include earlier ξ measurements for three samples with DS between 0.7 and 1.2 studied in (Lopez et al., 2015, 2018). These polymers were not part of this study.

Table 2 Equivalent conductances of counterions in water. Data from (Robinson and Stokes, 2002; Adamson, 1979).

Ion	λ_C [mS/M]
Li^+	38.7
Na^+	50.1
K^+	73.5
Cs^+	76.8
Mg^{2+}	53.05

The scattering profiles of NaCMC in DI water, whether measured by SANS or SAXS showed clear correlation peaks(Horkay and Hammouda, 2008; Dobrynin et al., 1995) over the entire concentration range studied, in agreement with earlier studies.(Lopez et al., 2015, 2018; Sharratt et al., 2020; Gulati et al., 2024; Hou et al., 2024a) By contrast, the magnesium salts of CMC did not display correlation peaks, irrespective of degree of substitution or polymer concentration. Instead, a broad 'correlation shoulder' is observed. This feature is reminiscent of the scattering profiles observed for sodium hyaluronate in DI water solutions (Salamon et al., 2013) or polyelectrolytes with modest concentrations of added salts.(Spiteri, 1997; Sharratt et al., 2020; Nishida et al., 2002; Prabhu et al., 2003; Slim et al., 2022) A comparison between the scattering profiles two NaCMC and MgCMC solutions at $c = 2$ wt% is shown in Fig. 3. The concentration in units of repeating units per volume is $\simeq 5\%$ higher for the MgCMC solution.

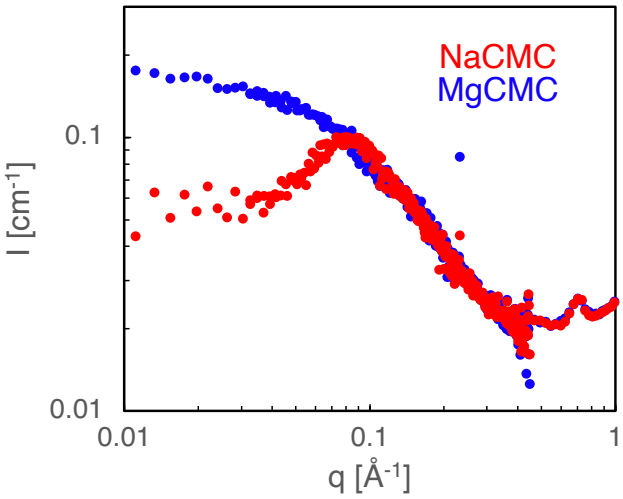

Fig. 3 Comparison of SAXS curves for sodium and magnesium salts of a solution of sample S2 in DI water. Both solutions are at a concentration of 2wt%. The data have been binned (3 to 1) for clarity.

Following the approach in (Salamon et al., 2013; Gulati et al., 2024; Hou et al., 2024a), we identify the cross-over between the high-q and intermediate q as the 'shoulder position'. We fit power-laws to the high-q and medium-q regions:

$$I(q) = \begin{cases} A_1 q^{m_1} & \text{if } q \lesssim q^* \\ A_2 q^{m_2} & \text{if } q \gtrsim q^* \end{cases} \tag{3}$$

where A_1, A_2, m_1 and m_2 are used as fit parameters and q^* is the wave-vector at which the two power-laws intersect. Examples of such fits to the magnesium salt of S1 at different polymer concentrations are shown in Fig. 4. The range over which the intermediate and high-q power laws were fit was identified visually, values for the various parameters are tabulated in the supporting information. Note that at high concentrations, the influence of the low-q upturn(Ermi and Amis, 1998; Lopez et al., 2024) on the mid-q scattering region becomes more important, which makes the power-law fits less reliable.

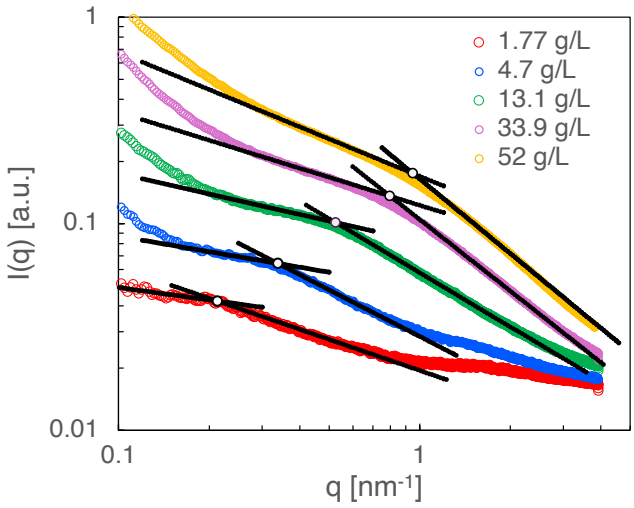

Fig. 4 Scattering profiles for S1 at different concentrations, indicated on the legend. Lines are fits to Eq. 3 and full circles indicate $(I(q^*), q^*)$ for each concentration.

The variation of the two exponents with concentration for the various MgCMC samples studied is plotted in Fig. 5. The values of m_1 and m_2 for each polymer sample studied are listed in the supporting information. No correlation with degree of substitution was observed. The pre-factors A_1 and A_2 were found to increase linearly with concentration, see the supporting information.

The chain conformation inside the correlation blob is expected to be rod-like because chains are strongly stretched by electrostatics, so that for $q \gtrsim 1/\xi$, the scattering intensity should scale as $I(q) \sim q^{-1}$. This dependence is consistent with SANS data from previous studies for NaCMC in aqueous solution. The value of m_2 plotted in Fig. 5, which describes the power-law of the scattering intensity for $q \gtrsim 2\pi\xi^{-1}$ decreases with concentration over the entire range studied. For low concentrations, the weaker than -1 exponent may be explained as arising from the contribution of the $q-$independent background scattering term, which is apparent, for example in the red curve in Fig. 4. At high concentrations, m_2 takes values lower than -1. The interpretation of this exponent is not obvious to us: bending inside the correlation blob is unlikely because for $c \gtrsim 0.07$ M, the correlation length becomes smaller than the bare Kuhn length. A possibility is that even at high q the contribution of the intermolecular structure factor remains significant, so that m_2 does not reflect the behaviour of the form factor of the chains inside the correlation blob.

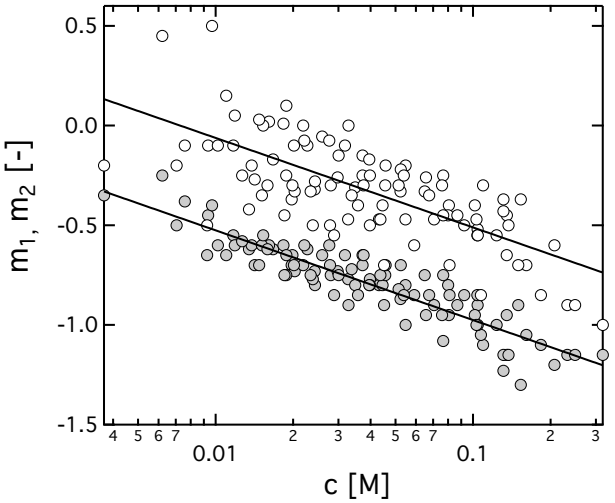

Fig. 5 Variation of m_1 (hollow symbols) and m_2 (full symbols) with concentration. Data include all samples studied. Lines are logarithmic lines to guide the eye.

Correlation length and the stretching parameter

The position of the correlation peak measured by SANS and SAXS yield identical values for NaCMC, see (Gulati et al., 2024). The correlation length was also shown to be independent of temperature(Lopez et al., 2015) and ion type for the alkali series.(Gulati et al., 2024) The degree of substitution has a weak or null influence on the position of the correlation peak of NaCMC solutions, except at very high concentrations because for low DS samples, a fraction of the polymer aggregates.(Lopez et al., 2018; Barba et al., 2002; Kamide et al., 1985)

The peak or shoulder positions (q^*) can be used to calculate the correlation length according to:

$$\xi = \frac{2\pi}{q^*}$$

The correlation length for the various sodium and magnesium salts of CMC studied is plotted as a function of concentration in Fig. 6. Both salts display a scaling of $\xi \sim c^{-1/2}$, in agreement with the theoretical prediction of the Dobrynin model. (Dobrynin et al., 1995) Note that for $c \gtrsim 0.035$ M for the sodium salt, the correlation length becomes smaller than the bare Kuhn length ($\simeq 10$ nm). For the magnesium salt, this cross-over occurs for $c \gtrsim 0.07$ M.

The scaling theory relates the correlation length to the stretching parameter B as:(Dobrynin et al., 1995)

$$\xi = \left(\frac{B}{bc}\right)^{1/2} \tag{4}$$

where b is the chemical monomer size, which is $\simeq 5$ Å for cellulose polymers and B is the stretching parameter, which describes the degree of chain coiling inside the correlation blob, with $B = 1$ corresponding to fully stretched chains and $B > 1$ to partial coiling.

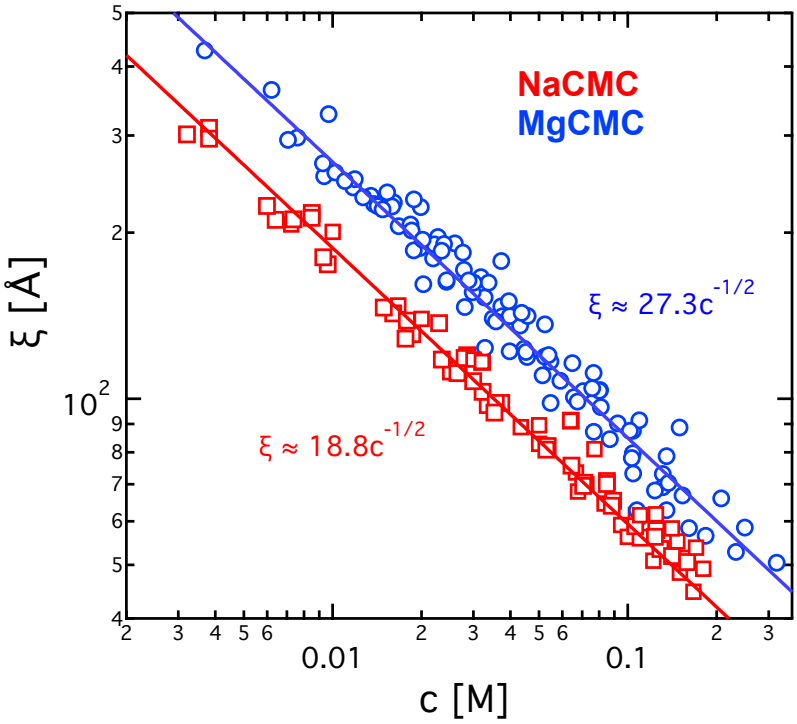

Fig. 6 Correlation length of sodium and magnesium salts of CMC in aqueous solution without added salts. Data for NaCMC are from refs (Lopez et al., 2015; Hou et al., 2025; Lopez et al., 2018; Sharratt et al., 2020; Gulati et al., 2024) and this work. Data for MgCMC are from this work. Lines are best-fit power-laws with the exponent fixed to -1/2.

The stretching parameter for NaCMC is found to be $B \simeq 1.1$ and for MgCMC $B \simeq 2.3$. This means that in dilute solution, NaCMC chains should have an end-to-end distance $\simeq 2.1\times$ larger than MgCMC. Based on this, we expect the overlap concentration of NaCMC to be $\simeq \times 2.1^3 \simeq 9$ lower than MgCMC, which contrasts with results from an earlier study(Lopez and Richtering, 2019), where viscosimetric estimates for the overlap concentrations of the sodium and magnesium salts of sample S1 found a ratio of 3.

The relatively large change in the stretching parameter with counterion valence contrasts with the independence of B on counterion type for monovalent counterions of the alkaline series.(Gulati et al., 2024) Similar results have been reported for polystyrene sulfonate (PSS): the correlation lengths of various alkali metal salts of PSS as well as its acid form were found to be nearly identical by Kaji and co-workers. By contrast, PSS with Mg^{2+} or Ca^{2+} counterions displays larger correlation lengths, corresponding to greater values of B.(Lopez et al., 2021; Combet et al., 2011, 2005) This phenomenon likely arises because the charge density of a polyelectrolyte is strongly dependent on the counterion valence, but not on the counterion size, see below.

Local conformation

Following our earlier work, SANS data were fitted to the worm-like chain model in the high q region using the following equation:(Lopez et al., 2015; Kassapidou et al., 1997)

$$I(q) = K\frac{\pi}{b'q}e^{-R_C^2q^2/4} + I_B \tag{5}$$

where K is a contrast factor, which is nearly identical for NaCMC and MgCMC due to the weak contrast between the counterions and the deuterated solvent background, b' is the $z-$projected monomer length, R_C is the chain's cross-sectional radius, which was set to 3.5 Å and I_B is a $q-$indpendent 'background' scattering intensity term.(Lopez et al., 2015)

Equation 5 was found in earlier work to give reasonable values for b' of NaCMC, see (Lopez et al., 2015, 2018). On the other hand, for MgPSS in aqueous solutions, we found that the extracted z-projected monomer length was similar to that of NaPSS, despite the more coiled concentration expected from the larger B parameter of MgPSS compared to NaPSS.(Lopez et al., 2021) Applying Eq. 5 to NaCMC and MgCMC samples at the same concentration suggests a higher value of b' for MgCMC than NaCMC. This is inconsistent with the measured B parameter and the fact that the NaCMC chain seems to be fully stretched inside the correlation blob. We do not have an explanation for this.

Low-q upturn

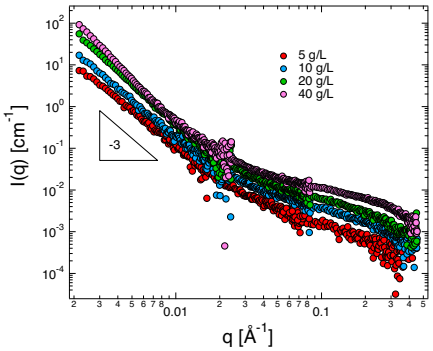

Fig. 7 Background subtracted SANS intensity MgCMC with different concentrations. Low-q upturn displays a power-law of $I(q) \propto q^{-3}$, indicated by the triangle.

In the low-q region ($\lesssim 0.01$Å^{-1}), the scattering intensity from the SAXS capillaries was too high to allow for reliable background subtraction. SANS measurements on the other hand allow for the low$-q$ intensity to be measured with high accuracy. SANS curves for MgCMC in D_2O measured at the D11 beamline are shown in Fig. 7. For all concentrations, an upturn in the low$-q$ region of the spectra is observed. The power-law of $\simeq -3$ is typical for mass fractals. This power-law exponent is lower (less negative) than the value of -3.6 found for NaCMC in DI water in previous studies.(Lopez et al., 2015; Gulati et al., 2024) The curves measured at the NGB30m source display a slightly higher power-law which is in better agreement with the exponent observed for NaCMC in earlier studies, see the

supporting information. The difference in exponents between the two sets of experiments suggests that sample preparation procedures influence the low-q exponent.

Conductivity

Aqueous solutions of NaCMC and MgCMC polymers with various degrees of substitution were prepared at concentrations around 20-30 g/L, as higher concentrations were too viscous for accurate conductivity measurement. Dilutions by a factor of $\simeq \times 1.5$ were then performed for each sample, and the conductivity of each sample was recorded at its respective concentration. This dilution process continued until the conductivity approached approximately 20 μS/cm. At this point, the conductivity is only $\simeq 7-10$ higher than that of the solvent and estimates of the specific conductance become unreliable. All measurements were conducted at a controlled temperature of 25 ± 0.05°C, with a water bath ensuring thermal stability. Thermogravimetric analysis (TGA) was used to quantify the residual moisture in CMC samples. TGA revealed that the average moisture content in these samples were $\simeq 13\%$ and 15% for NaCMC and MgCMC respectfully and the values didn't show any impact of the degree of substitution, see Fig. S2. The value of the water content were used to adjust the actual concentrations of CMC solutions.

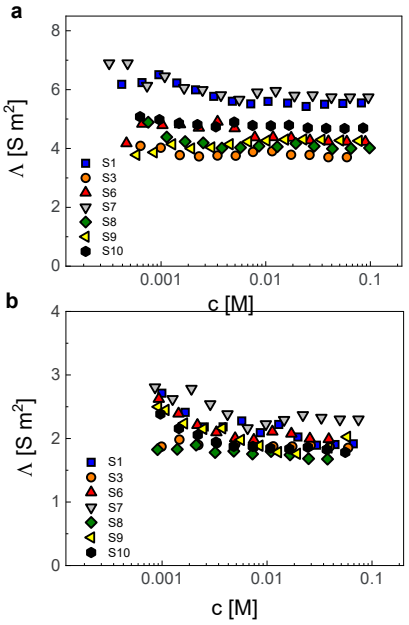

Fig. 8 Conductance of carboxymethyl cellulose with different degree of substitution as a function of concentration a: with monovalent counterion (NaCMC) b: with divalent counterion (MgCMC).

Figure 8 shows the specific conductance ($\Lambda = \kappa/c$) of CMC polymers as a function of concentration with monovalent and divalent counterions. The CMC polymers have a degree of substitution (DS) ranging from 0.72 to 1.4. At lower concentrations, an upturn in the

chemical conductivity is seen which can be due to the existence of residual salts in the solution. With increasing concentration, the conductance levels off at a constant value since the interference of the residual salt is less important.

As the degree of substitution in NaCMC increases (Fig8a), we observe a corresponding increase in the electrical conductivity of NaCMC. Sample S3 with DS = 0.72 has the lowest chemical charge density of an ionic group per 7 Å ($u \simeq 1$), and S7 (DS = 1.4) has the highest chemical charge density of an ionic group per 3.5 Å ($u \simeq 2$). While the chemical charge density doubles from S3 to S7, the conductance does not increase proportionally. This is because condensed counterions neutralize some of the charged groups on the backbone, suppressing the overall charge density and electrical conductivity of the solution.

The model of Colby et al gives the specific conductance of a salt-free polyelectrolyte solution as:

$$\Lambda = f\left[\lambda_C + f\frac{N_A^2 z_C \xi^2 e^2 ln(\xi/D)}{3\pi\eta_s}\right] \tag{6}$$

where z_C the valence of the counterion, ξ is the correlation length, D is the cross-sectional diameter of the chain, η_s the viscosity of the solvent, c_m is the polymer concentration in moles of monomers per volume, and f is the fraction of monomers with a dissociated counterion. The concentration of free counterions is fc/z. λ_C is the equivalent conductance the counterion in units of Sm^2/mol, $\lambda_C = \lambda'_C/z_C$, where λ'_C is the molar conductance of the counterion.

Equation 6 is a quadratic equation in f. Knowing the values of ξ, D and the various constants, f can be calculated for any concentration from the measured value of Λ.

Influence of counterion type

Figure 9 plots the fraction of monomers with a dissociated counterion for sample S2 (DS $\simeq$ 0.9) with different alkaline metal counterions. All four salts show a slow increase in the fraction of ionised monomers with concentration. The value of f depends weakly on the counterion type, with the difference between LiCMC and CsCMC being $\simeq$ 20%. The order of counterion dissociation observed for the alkaline earth counterions is qualitatively consistent with the model of Oosawa, which expects that larger counterions dissociate to a greater extent and also with that of Ghosh and Kundagrami (Ghosh and Kundagrami, 2024). Our results are also in line with studies by various groups using electrical conductivity (Trivedi and Patel, 1986; Milas, 1969, 1974) and osmotic pressure.(Milas, 1974)

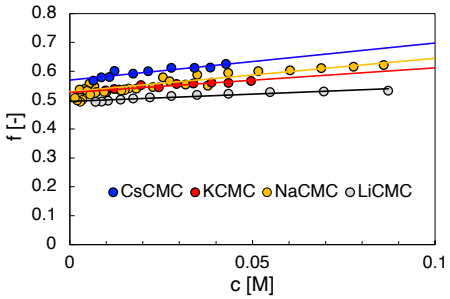

Fig. 9 Fraction of monomers bearing a dissociated charge as a function of concentration for different alkaline metal salts of S2. Lines are guides to the eye. Data for NaCMC combine results from this work and (Hou et al., 2024a).

Despite the large differences in site-binding strength for the alkaline metal counterions which are apparent from the ultrasound absorption measurements by Milas and coworkers(Milas, 1974; Zana et al., 1971) (fig 2a), their influence in counterion condensation are minimal. This suggests that site-binding for the CMC-alkaline metal system does not induce counterion condensation. Instead, site-bound counterions are a sub-set of condensed counterions. Some evidence against this view can be found in the activity coefficient of K^+ counterions in ionic derivatives of Dextran (Satake et al., 1972; Noguchi et al., 1973). This may be a peculiarity of branched polyelectrolytes or it may reflect the stronger site-binding strength of alkaline ions to dextran derivatives.

Influence of degree of substitution and counterion valence on the fraction of free counterions

Figure 10 shows the fraction of monomers with a dissociated counterion as a function of concentration across different degrees of substitution. The correlation length at each polymer concentration is calculated from the data in Fig. 6: $\xi = 18.8c^{-1/2}$ for NaCMC, and $\xi = 27.3c^{-1/2}$ for MgCMC, independent of DS. By incorporating the correlation length and the conductivity at each concentration into Eq. 6, the fraction of monomers bearing a dissociated charge is calculated. We choose a value of $D = 7$ Å for the cross-sectional diameter of chains, independent of DS. (Lopez et al., 2015, 2018). For all degrees of substitution, the fraction of free counterions is found to follow an approximately linear relationship with concentration, see also fig 9.

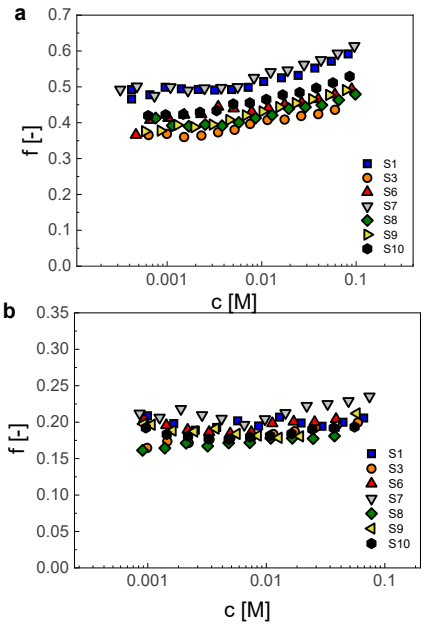

Fig. 10 a: Conductance of NaCMC with different DS values as a function of polymer concentration b: Fraction of charged monomers for various samples as a function of polymer concentration. Values of f are calculated with Eq. 6 and the ξ data from Fig. 6.

According to Oosawa-Manning condensation theory, polyelectrolytes with high charge densities, in dilute solutions, have an effective charge density of $\mu_{eff} = e/l_B$, i.e. one charge per Bjerrum length along the chain contour. With this assumption, Oosawa-Manning predicts that fraction of monomers bearing a dissociated charge is $f = b_c/(z_C l_B)$ where b_c is the distance between ionic groups along the backbone, which can be considered either as the monomer length ($b \simeq 5.15$ Å), or the monomer length divided by the stretching parameter (b/B). For NaCMC, the stretching parameter obtained by SAXS and SANS analysis is $\simeq 1.1$, independent of degree of substitution.(Lopez et al., 2018) The Oosawa-Manning threshold corresponds to DS $\simeq 0.6-0.7$ for NaCMC in water.

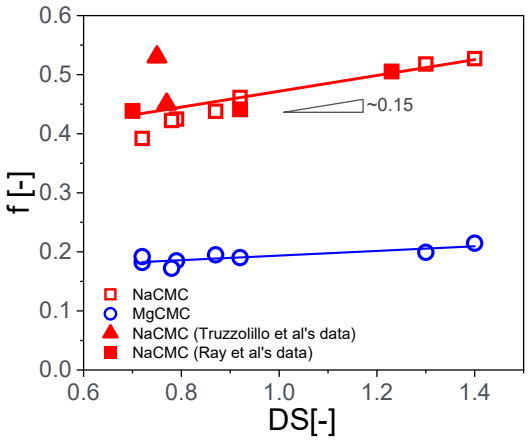

Fig. 11 Fraction of monomers bearing a dissociated charge as a function of degree of substitution. Hollow symbols are from this work and full symbols evaluate f from the conductivity data of Ray et al extrapolated to $T = 25$ ° C using the same method as for our samples. Estimates for f by Truzzzolillo et al, based on solution conductivity but employing a different method to calculate f are also included for comparison. Red symbols are for NaCMC and blue symbols for MgCMC.

At concentrations below 0.01 M, we can see a an approximately constant value for f, varying from 0.34 for DS = 0.72 to 0.5 for DS = 1.4. The counterion fraction at DS = 1.4 is close to Oosawa-Manning predictions (0.6) but deviates further away as the degree of substitution decreases. At the lowest degree of substitution, DS $\simeq 0.7$, the Oosawa-Manning theory expects no counterion condensation (i.e. $f \simeq$ DS) but the measured value of f approximately half of this value. The discrepancy may arise, at least in part, due to the heterogeneity of substitution of the polymer: for a homogeneously substituted sample with DS $\simeq 0.7$, the spacing between each charge is equal to the Bjerrum length and no condensation is expected. If substitution heterogeneous, regions of high substitution co-exist with less substituted ones. In the more substituted regions, the charge spacing will be smaller than l_B leading to condensation. This provides a plausible explanation for why condensation is observed in heterogeneous systems even when the *average* charge spacing is larger than the l_B. The average value of f, for divalent MgCMC, is calculated to be $f \simeq 0.2$, $\times \simeq 2$ lower than the value for NaCMC, in agreement with Oosawa-Manning theory.

Figure 11 compares how the degree of substitution influences the fraction of free counterions in Na and MgCMC. In both cases, a linear dependence of f on the degree of substi-

tution is observed, with the slope for the sodium salts being larger than for MgCMC. The weak influence of DS on the fraction of charged monomers contrasts with the large influence DS has on chain dynamics: for $DS \lesssim 0.9$, associative interactions between chains become important at high concentrations ($c \gtrsim 0.05$ M), leading to physical gelation.(Elliot and Ganz, 1974; Lopez et al., 2018; Lopez and Richtering, 2021) Such associations appear to have no clear influence on the fraction of dissociated counterions or the polyion conductivity.

The conductivity data of Ray et al(Ray et al., 2016) for solutions of NaCMC in DI water were extrapolated to $T = 25$ °C and used to evaluate f by the same procedure as for our data. The results are in good agreement with our data. Truzzolillo et al estimate the charge fraction of NaCMC based on conductivity data but using a different procedure than the one employed here. Their results for two NaCMC polymers are plotted in Fig. 11 as red triangles. One of their samples agrees well with our results while the other displays a value of $f \simeq$ 20% higher than the other estimates.

Table 3 Comparison of estimates for the fraction of charged monomers for CMC with DS $\simeq$ 1.2-1.3 according to different methods. [a] Based on applying Dobrynin's quantitative scaling to salt-free viscosity data [b] Based on applying Dobrynin et al's 1995 scaling model to the decrease of solution viscosity with added salt. [c] Values are interpolated to DS = 1.3 from data in fig 1. Estimates of f are using Oosawa's model which equates counterion activity with f. [d] interpolated from data in the DS = 1.1-2.5 range. [e] Approximated from Rinaudo et al's result for CaCMC with DS = 1.6, assuming the charge fraction is the same as DS = 1.3. Osmometry estimates for f are obtained assuming each dissociated counterion contributes k_BT to the osmotic pressure and condensed counterions are osmotically inactive.

Method	DS $\simeq$ 1.3		DS $\simeq$ 0.8		Refs.
	f_{Na}	f_{Mg}	f_{Na}	f_{Mg}	
Conductivity	0.5	0.22	0.45	0.2	This work, (Ray et al., 2016)
Ion selective potentiometry[c]	0.72	0.3	0.58	–	(Rinaudo and Loiseleur, 1973; Rinaudo et al., 1971; Rinaudo and Milas, 1974; Rinaudo and Mils, 1978; Rinaudo, 1973; Rinaudo and Milas, 1975; Nagasawa and Kagawa, 1957), see Fig. 1.
Vapour pressure osmometry	0.67[d]	–	–	–	(Rinaudo and Loiseleur, 1973; Rinaudo and Milas, 1975)
Membrane osmometry	0.69[d]	0.37[e]	–	–	(Rinaudo and Loiseleur, 1973; Rinaudo and Milas, 1975)
Dielectric Spectroscopy[a]	–	–	0.3	–	(Truzzolillo et al., 2009)
Viscosity[b]	0.42	–	–	–	(Lopez et al., 2017; Matsumoto et al., 2025)
Viscosity[a]	0.15	0.09	–	–	(Jacobs et al., 2021)

Comparison of methods to estimate counterion condensation

The conductivity data from this study and others yield consistent results for the fraction of charged monomers of NaCMC. Next, we try to establish wether different methods of estimating the fraction of free counterions also yield consistent results. We assume that the counterion activity and the osmotic coefficient of the counterions is equal to the fraction of free counterions. This corresponds to the Oosawa theory.(Oosawa, 1971) These values are in quantitative agreement with the conductivity data for sodium and magnesium salts of CMC with DS = 1.3 and 0.8. A possible explanation is as follows: the model of Colby et al assumes that free (non-condensed) counterions have the same mobility as in a solution of a simple salt, but experimental measurements, in agreement with theoretical predictions

show that free polyelectrolyte counterions have a diffusion coefficient $\simeq 30\%$ lower than that of the ion in simple salt solutions.(Ander and Kardan, 1984) If the mobility in Eq. 6 is adjusted by a similar pre-factor, the conductivity estimates for f_{Na} and f_{Mg} increase by $\simeq 10-15\%$, bringing them closer to the potentiometry and osmometry estimates. Given the limited osmotic pressure data, experimental error should not be ruled out as a possible cause of the disagreement.

Bordi et al. used the following equation to evaluate the fraction of charged monomers from dielectric spectroscopy data:(Bordi et al., 2004)

$$f = \frac{\Delta\varepsilon}{6\pi\omega_C D_{CI} l_B \varepsilon c} \tag{7}$$

here $\Delta\varepsilon$ is the dielectric increment and ω_C the characteristic frequency of the intermediate relaxation decay, see (Bordi et al., 2004). D_{CI} is the diffusion coefficient of the counterion (1.3×10^{-9} m^2/s).

Using the dielectric spectroscopy data of Truzzolillo et al(Truzzolillo et al., 2009), we estimate $f \simeq 0.3$ for their two samples with DS $\simeq 0.8$. The value from Eq. 7 is lower than the conductivity and potentiometric estimates for NaCMC with this DS. This contrasts with the NaPSS system, where Bordi et al showed that Eq. 7 gives f values which are $\simeq \times\ 5$ higher than those from conductivity and osmotic pressure data.

The fraction of charged monomers obtained from the decrease in NaCMC solutions upon salt addition obtained by Matsumoto et al.(Matsumoto et al., 2025) agrees reasonably well with our conductivity estimate. By contrast the viscosimetric estimate from Dobrynin's quantitative scaling appears too low.(Jacobs et al., 2021)

In summary, the various methods considered yield results which agree qualitatively. Due to the limited data available for all methods other than conductivity, it is not possible, at present, to draw any solid conclusions on the reasons for the lack of quantitative agreement.

Transference number

The transference number of the polyion (t_p) was determined using the equivalent conductivity of the solution and the polyion mobility (λ_p) calculated from the model of Colby et al:

$$t_p = \left(\frac{\lambda_p}{\Lambda}\right) \tag{8}$$

Figure 12 shows the transference number of the polyion plotted against the equivalent concentration of the polyelectrolyte for all samples. The transference number values of the polyion for MgCMC were found to exceed unity, with the value of $\sim$3 at lower concentrations and leveling off to a value closer to 2 at higher concentration, while NaCMC samples have a transference number closer to unity. It is well established that the transference number is highly dependent on the polyion's charge density—higher charge density typically results in a higher transference number. The transference numbers indicate that a significant fraction of the counterions migrate in the same direction as the polyions. The conductivity of the CMCs with divalent counterion results primarily from the polyion while in monovalent case both polyion and counter ion have similar contribution to the solution conductivity.

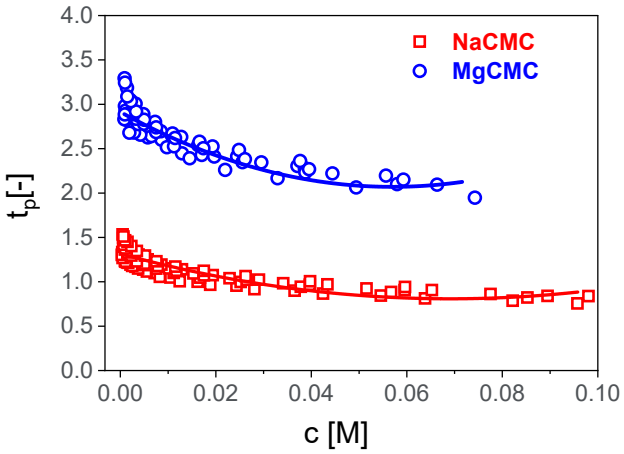

Fig. 12 Transference number of the polyion (t_p) in aqueous carboxymethylcellulose solutions with a mono (NaCMC) and divalent (MgCMC) counterions as a function of the polyelectrolyte concentration. The lines fitted to the data points are to demonstrate the trend.

Conclusions

This study examined the effects of counterion type and charge density on the structural and electrostatic properties of carboxymethyl cellulose (CMC) in aqueous solutions. Small-angle X-ray and neutron scattering (SAXS/SANS) reveal distinct structural differences between NaCMC and MgCMC. MgCMC solutions lacked the well-defined correlation peaks seen for NaCMC, instead displaying broad scattering shoulders, which suggests a less ordered local structure due to weaker electrostatic repulsion. While NaCMC chains remained locally extended (with a stretching parameter $B \simeq 1.1$), MgCMC exhibited significant coiling ($B \simeq 2.3$).

Electrical conductivity measurements further elucidate the role of counterion valence in charge screening. The fraction of charged monomers f was consistently higher for NaCMC (0.4–0.5) than for MgCMC (0.19–0.21), in quantitative agreement with the Oosawa-Manning theory, which expects the charge fraction to vary inversely with the counterion valence. However, the experimental values of f fall below theoretical predictions, particularly for low-DS samples, perhaps due to the heterogeneous distribution of charged groups along the CMC backbone. While monovalent alkali counterions (Li^+ to Cs^+) show only minor variations in f, despite differences in site-binding affinity, the switch from Na^+ to Mg^{2+} resulted in a sharp decline in charge dissociation, highlighting the dominant role of valence over ion-specific effects in condensation.

Acknowledgements

We are grateful to the Spring-8 synchrotron and NIST center for neutron research for beamtime. We thank Dr. Noboru Ohta for his assistance at SPring-8 beamline BL40B2, in support of the experiments under proposal number 2024A1203. We would also like to thank Bahar Baniasadi (PSU) Prof. Atsushi Matsumoto (University of Fukui), Himari Taniguchi, Marina

Ikeda, Yume Tao, Rene Iwato, Hikari Tsunekawa, Hinako Nakayama, Kyoka Hinomoto, Taiki Okamoto, Naruki Kanda (Okayama University), Anish Gulati and Hannes Luhmann (RWTH) for their contribution in sample preparation and measurements at BL40B2. We are grateful for Dow and CP Kelco for donating NaCMC polymers. We thank Will Sharratt (University of Liverpool) and Joao Cabral (Imperial College London) for measuring SANS samples at the D11 beamline. We thank Andrey Dobrynin (UNC Chapel Hill) for useful discussions and for providing feedback on a draft of the manuscript. This work was partially supported by JSPS KAKENHI Grant Number JP24K01236 and JP20KK0325. F.H. acknowledges the support of the Intramural Research Program of the Eunice Kennedy Shriver National Institute of Child Health and Human Development, National Institutes of Health. CGL acknowledges funding from the DFG, project number GO 3250/2-1.

Author contributions

E.A.: Experimental measurements, data analysis, writing, editing **T.W.:** Experiments, funding, beamtime proposal writing, writing, editing. **F.H.:** Experiments, proposal writing, data interpretation **C.H.:** Experiments, beamtime proposal writing, writing, editing. **C.G.L:** Experiments, beamtime proposal writing, funding, data analysis and interpretation, writing, editing **M.H.:** Experiments, beamtime proposal writing, data analysis and interpretation, writing, editing.

References

Adamson, A. (1979). *A textbook of physical chemistry*. Elsevier.

Agrawal, A., Radakovic, A., Vonteddu, A., Rizvi, S., Huynh, V. N., Douglas, J. F., Tirrell, M. V., Karim, A., and Szostak, J. W. (2024). Did the exposure of coacervate droplets to rain make them the first stable protocells? *Science Advances*, 10(34):eadn9657.

Ander, P. and Kardan, M. (1984). Interactions of sodium ions with polyelectrolytes of varying charge density. *Macromolecules*, 17(11):2431–2436.

Arumughan, V., Ozeren, H. D., Hedenqvist, M., Skepo, M., Nypelo, T., Hasani, M., and Larsson, A. (2023). Anion-specific adsorption of carboxymethyl cellulose on cellulose. *Langmuir*, 39(42):15014–15021.

Barba, C., Montané, D., Rinaudo, M., and Farriol, X. (2002). Synthesis and characterization of carboxymethylcelluloses (cmc) from non-wood fibers i. accessibility of cellulose fibers and cmc synthesis. *Cellulose*, 9:319–326.

Behra, J. S., Mattsson, J., Cayre, O. J., Robles, E. S., Tang, H., and Hunter, T. N. (2019). Characterization of sodium carboxymethyl cellulose aqueous solutions to support complex product formulation: A rheology and light scattering study. *ACS Applied Polymer Materials*, 1(3):344–358.

Beyer, D. and Holm, C. (2024). Unexpected two-stage swelling of weak polyelectrolyte brushes with divalent counterions. *ACS Macro Letters*, 13(9):1185–1191.

Bordi, F., Cametti, C., and Colby, R. (2004). Dielectric spectroscopy and conductivity of polyelectrolyte solutions. *Journal of Physics: Condensed Matter*, 16(49):R1423.

Buvalaia, E., Kruteva, M., Hoffmann, I., Radulescu, A., Forster, S., and Biehl, R. (2023). Interchain hydrodynamic interaction and internal friction of polyelectrolytes. *ACS Macro Letters*, 12(9):1218–1223.

Cai, Y., Li, D., Peng, S., and Liu, H. (2025). Synthesis of dual-responsive carboxymethyl cellulose–based nanogels for drug delivery applications. *Colloid and Polymer Science*, 303(2):287–300.

Carrillo, J.-M. Y. and Dobrynin, A. V. (2011). Polyelectrolytes in salt solutions: Molecular dynamics simulations. *Macromolecules*, 44(14):5798–5816.

Chang, R. and Yethiraj, A. (2003). Brownian dynamics simulations of polyelectrolyte solutions with divalent counterions. *The Journal of chemical physics*, 118(24):11315–11325.

Chen, G., Perazzo, A., and Stone, H. A. (2021). Electrostatics, conformation, and rheology of unentangled semidilute polyelectrolyte solutions. *Journal of Rheology*, 65(4):507–526.

Chremos, A. and Douglas, J. F. (2016). Influence of higher valent ions on flexible polyelectrolyte stiffness and counter-ion distribution. *The Journal of chemical physics*, 144(16).

Chremos, A. and Douglas, J. F. (2017). Communication: Counter-ion solvation and anomalous low-angle scattering in salt-free polyelectrolyte solutions. *The Journal of chemical physics*, 147(24).

Chremos, A. and Douglas, J. F. (2018). Polyelectrolyte association and solvation. *The Journal of chemical physics*, 149(16).

Colby, R. H. (2010). Structure and linear viscoelasticity of flexible polymer solutions: comparison of polyelectrolyte and neutral polymer solutions. *Rheologica acta*, 49:425–442.

Collins, K. D. (2004). Ions from the hofmeister series and osmolytes: effects on proteins in solution and in the crystallization process. *Methods*, 34(3):300–311.

Combet, J., Isel, F., Rawiso, M., and Boué, F. (2005). Scattering functions of flexible polyelectrolytes in the presence of mixed valence counterions: condensation and scaling. *Macromolecules*, 38(17):7456–7469.

Combet, J., Rawiso, M., Rochas, C., Hoffmann, S., and Boué, F. (2011). Structure of polyelectrolytes with mixed monovalent and divalent counterions: Saxs measurements and poisson- boltzmann analysis. *Macromolecules*, 44(8):3039–3052.

Diederichsen, K. M., Terrell, R. C., and McCloskey, B. D. (2019). Counterion transport and transference number in aqueous and nonaqueous short-chain polyelectrolyte solutions. *The Journal of Physical Chemistry B*, 123(50):10858–10867.

Dobrynin, A. V., Colby, R. H., and Rubinstein, M. (1995). Scaling theory of polyelectrolyte solutions. *Macromolecules*, 28(6):1859–1871.

Dobrynin, A. V. and Rubinstein, M. (2005). Theory of polyelectrolytes in solutions and at surfaces. *Progress in polymer science*, 30(11):1049–1118.

Dubois, E. and Boué, F. (2001). Conformation of poly (styrenesulfonate) polyions in the presence of multivalent ions: small-angle neutron scattering experiments. *Macromolecules*, 34(11):3684–3697.

Ehtiati, K., Moghaddam, S. Z., Klok, H.-A., Daugaard, A. E., and Thormann, E. (2022). Specific counterion effects on the swelling behavior of strong polyelectrolyte brushes. *Macromolecules*, 55(12):5123–5130.

Elliot, J. H. and Ganz, A. (1974). Some rheological properties of sodium carboxymethylcellulose solutions and gels. *Rheologica Acta*, 13(4):670–674.

Ermi, B. D. and Amis, E. J. (1998). Domain structures in low ionic strength polyelectrolyte solutions. *Macromolecules*, 31(21):7378–7384.

Essafi, W., Lafuma, F., and Williams, C. (1999). Structural evidence of charge renormalization in semi-dilute solutions of highly charged polyelectrolytes. *The European Physical Journal B-Condensed Matter and Complex Systems*, 9:261–266.

Ghosh, S. and Kundagrami, A. (2024). Effect of counterion size on polyelectrolyte conformations and thermodynamics. *The Journal of Chemical Physics*, 160(8).

Glisman, A., Mantha, S., Yu, D., Wasserman, E. P., Backer, S., and Wang, Z.-G. (2024). Multivalent ion-mediated polyelectrolyte association and structure. *Macromolecules*, 57(5):1941–1949.

Gregory, K. P., Elliott, G. R., Robertson, H., Kumar, A., Wanless, E. J., Webber, G. B., Craig, V. S., Andersson, G. G., and Page, A. J. (2022). Understanding specific ion effects and the hofmeister series. *Physical Chemistry Chemical Physics*, 24(21):12682–12718.

Gulati, A., Douglas, J. F., Matsarskaia, O., and Lopez, C. G. (2024). Influence of counterion type on the scattering of a semiflexible polyelectrolyte. *Soft Matter*, 20(43):8610–8620.

Gulati, A., Jacobs, M., Lopez, C. G., and Dobrynin, A. V. (2023). Salt effect on the viscosity of semidilute polyelectrolyte solutions: sodium polystyrenesulfonate. *Macromolecules*, 56(5):2183–2193.

Hedlund, A. and Germgård, U. (2007). Some aspects on the kinetics of etherification in the preparation of cmc. *Cellulose*, 14:161–169.

Hemmes, P. (1972). Volume changes of ionic association reactions. *The Journal of Physical Chemistry*, 76(6):895–900.

Hen, J. and Strauss, U. P. (1974). Counterion binding by poly (vinyl sulfonate). *The Journal of Physical Chemistry*, 78(10):1013–1017.

Hirotsu, S. (1994). Static and time-dependent properties of polymer gels around the volume phase transition. *Phase Transitions: A Multinational Journal*, 47(3-4):183–240.

Horkay, F. and Douglas, J. F. (2025). Effect of divalent ions on the structure of polyelectrolyte gels. *Polymer*, 327:128311.

Horkay, F. and Hammouda, B. (2008). Small-angle neutron scattering from typical synthetic and biopolymer solutions. *Colloid and Polymer Science*, 286:611–620.

Hotton, C., Ducouret, G., Sirieix-Plénet, J., Bizien, T., Porcar, L., and Malikova, N. (2023). Tuning structure and rheological properties of polyelectrolyte-based hydrogels through counterion-specific effects. *Macromolecules*, 56(3):923–933.

Hotton, C., Sakhawoth, Y., Rollet, A.-L., Sirieix-Plénet, J., Tea, L., Combet, S., Sharp, M., Hoffmann, I., Nallet, F., and Malikova, N. (2024). Ion-specific effects in polyelectrolyte solutions: chain–chain interactions, chain rigidity and dynamics. *Comptes Rendus. Chimie*, 27(S5):1–13.

Hou, C., Watanabe, T., Lopez, C. G., and Richtering, W. (2024a). Structure and rheology of carboxymethylcellulose in polar solvent mixtures. *Carbohydrate Polymers*, page 122287.

Hou, C., Watanabe, T., Lopez, C. G., and Richtering, W. (2025). Structure and rheology of carboxymethylcellulose in polar solvent mixtures. *Carbohydrate Polymers*, 347:122287.

Hou, J., Chang, H., Liu, Y., Zhang, H., Li, H., Wang, Z., Rayan, A. M., Ghamry, M., Mohamed, T. A., and Zhao, K. (2024b). Exploring the phase behavior of natural egg yolk-carboxymethyl cellulose concentrate: Impact on emulsification and gelling properties. *Food Hydrocolloids*, 157:110385.

Jacobs, M., Lopez, C. G., and Dobrynin, A. V. (2021). Quantifying the effect of multivalent ions in polyelectrolyte solutions. *Macromolecules*, 54(20):9577–9586.

Jimenez, L. N., Martínez Narváez, C. D., and Sharma, V. (2020). Capillary breakup and extensional rheology response of food thickener cellulose gum (nacmc) in salt-free and excess salt solutions. *Physics of Fluids*, 32(1).

Jimenez, L. N., Martinez Narvaez, C. D., and Sharma, V. (2022). Solvent properties influence the rheology and pinching dynamics of polyelectrolyte solutions: Thickening the pot with glycerol and cellulose gum. *Macromolecules*, 55(18):8117–8132.

Kaji, K., Urakawa, H., Kanaya, T., and Kitamaru, R. (1984). Distance distribution analysis of small-angle x-ray scattering for semidilute polyelectrolyte solutions without salts. *Macromolecules*, 17(9):1835–1839.

Kamide, K., Okajima, K., Kowsaka, K., Matsui, T., Nomura, S., and Hikichi, K. (1985). Effect of the distribution of substitution of the sodium salt of carboxymethylcellulose on its absorbency toward aqueous liquid. *Polymer Journal*, 17(8):909–918.

Kassapidou, K., Jesse, W., Kuil, M., Lapp, A., Egelhaaf, S., and Van der Maarel, J. (1997). Structure and charge distribution in dna and poly (styrenesulfonate) aqueous solutions. *Macromolecules*, 30(9):2671–2684.

Kherb, J., Flores, S. C., and Cremer, P. S. (2012). Role of carboxylate side chains in the cation hofmeister series. *The Journal of Physical Chemistry B*, 116(25):7389–7397.

Kim, Y., Kim, S., Kim, B. S., Park, J. H., Ahn, K. H., and Park, J. D. (2022). Yielding behavior of concentrated lithium-ion battery anode slurry. *Physics of Fluids*, 34(12).

Koda, S., Sugi, Y., Sakurai, T., Matsuoka, T., and Nomura, H. (2004). Study on segmental motion and ion binding in polyelectrolyte solutions by ultrasonic spectroscopy. *Journal of solution chemistry*, 33:747–760.

Komiyama, J., Ando, M., Takeda, Y., and Iuma, T. (1976). Dilatometric study of monovalent counter-ion association with carboxylates. *European Polymer Journal*, 12(3):201–207.

Komiyama, J., Takeda, Y., Ando, M., and Iijima, T. (1974). Dilatometric study of monovalent counter-ion association with polymethacrylate. *Polymer*, 15(7):468–470.

Kondou, S., Sakashita, Y., Morinaga, A., Katayama, Y., Dokko, K., Watanabe, M., and Ueno, K. (2023). Concentrated nonaqueous polyelectrolyte solutions: High na-ion transference number and surface-tethered polyanion layer for sodium-metal batteries. *ACS Applied Materials & Interfaces*, 15(9):11741–11755.

Kong, P., Rosnan, S. M., and Enomae, T. (2024). Carboxymethyl cellulose–chitosan edible films for food packaging: A review of recent advances. *Carbohydrate polymers*, page 122612.

Kono, H., Oshima, K., Hashimoto, H., Shimizu, Y., and Tajima, K. (2016a). Nmr characterization of sodium carboxymethyl cellulose 2: Chemical shift assignment and conformation analysis of substituent groups. *Carbohydrate Polymers*, 150:241–249.

Kono, H., Oshima, K., Hashimoto, H., Shimizu, Y., and Tajima, K. (2016b). Nmr characterization of sodium carboxymethyl cellulose: Substituent distribution and mole fraction of monomers in the polymer chains. *Carbohydrate Polymers*, 146:1–9.

Legrand, G., Baeza, G. P., Peyla, M., Porcar, L., Fernández-de Alba, C., Manneville, S., and Divoux, T. (2024). Acid-induced gelation of carboxymethylcellulose solutions. *ACS Macro Letters*, 13(2):234–239.

Liao, Q., Carrillo, J.-M. Y., Dobrynin, A. V., and Rubinstein, M. (2007). Rouse dynamics of polyelectrolyte solutions: Molecular dynamics study. *Macromolecules*, 40(21):7671–7679.

Liao, Q., Dobrynin, A. V., and Rubinstein, M. (2003). Molecular dynamics simulations of polyelectrolyte solutions: osmotic coefficient and counterion condensation. *Macromolecules*, 36(9):3399–3410.

Liu, Y. and Zhao, K. (2019). Rheological and dielectric behavior of milk/sodium carboxymethylcellulose mixtures at various temperatures. *Journal of Molecular Liquids*, 290:111175.

Lopez, C. G. (2020). Entanglement of semiflexible polyelectrolytes: Crossover concentrations and entanglement density of sodium carboxymethyl cellulose. *Journal of Rheology*, 64(1):191–204.

Lopez, C. G., Colby, R. H., and Cabral, J. T. (2018). Electrostatic and hydrophobic interactions in nacmc aqueous solutions: Effect of degree of substitution. *Macromolecules*, 51(8):3165–3175.

Lopez, C. G., Colby, R. H., Graham, P., and Cabral, J. T. (2017). Viscosity and scaling of semiflexible polyelectrolyte nacmc in aqueous salt solutions. *Macromolecules*, 50(1):332–338.

Lopez, C. G., Horkay, F., Schweins, R., and Richtering, W. (2021). Solution properties of polyelectrolytes with divalent counterions. *Macromolecules*, 54(22):10583–10593.

Lopez, C. G., Matsumoto, A., and Shen, A. Q. (2024). Dilute polyelectrolyte solutions: recent progress and open questions. *Soft Matter*.

Lopez, C. G. and Richtering, W. (2019). Influence of divalent counterions on the solution rheology and supramolecular aggregation of carboxymethyl cellulose. *Cellulose*, 26:1517–1534.

Lopez, C. G. and Richtering, W. (2021). Oscillatory rheology of carboxymethyl cellulose gels: Influence of concentration and ph. *Carbohydrate Polymers*, 267:118117.

Lopez, C. G., Rogers, S. E., Colby, R. H., Graham, P., and Cabral, J. T. (2015). Structure of sodium carboxymethyl cellulose aqueous solutions: A sans and rheology study. *Journal of Polymer Science Part B: Polymer Physics*, 53(7):492–501.

Lytle, T. K., Muralidharan, A., and Yethiraj, A. (2021). Why lithium ions stick to some anions and not others. *The Journal of Physical Chemistry B*, 125(17):4447–4455.

Manning, G. S. (1969). Limiting laws and counterion condensation in polyelectrolyte solutions i. colligative properties. *The journal of chemical Physics*, 51(3):924–933.

Manning, G. S. (1974). Limiting laws for equilibrium and transport properties of polyelectrolyte solutions. In *Polyelectrolytes: Papers Initiated by a NATO Advanced Study Institute on Charged and Reactive Polymers held in France, June 1972*, pages 9–37. Springer.

Marcus, Y. and Hefter, G. (2006). Ion pairing. *Chemical reviews*, 106(11):4585–4621.

Marioni, N., Rajesh, A., Zhang, Z., Freeman, B. D., and Ganesan, V. (2024). What is the influence of ion aggregation and counterion condensation on salt transport in ion exchange membranes? *Journal of Membrane Science*, 701:122713.

Matsumoto, A., Ikeda, M., Sugihara, S., and Maeda, Y. (2025). Viscometric method for estimating the charge fraction of polyelectrolytes in solutions. *Nihon Reoroji Gakkaishi*, 53(1):1–10.

Matsumoto, A., Ukai, R., Osada, H., Sugihara, S., and Maeda, Y. (2022). Tuning the solution viscosity of ionic-liquid-based polyelectrolytes with solvent dielectric constants via the counterion condensation. *Macromolecules*, 55(23):10600–10606.

Milas, M. (1969). *Fixation sélective des cations sur un polyélectrolyte anionique*. PhD thesis, Université de Grenoble.

Milas, M. (1974). *Intéraction avec les cations compensateurs et sélectivité ionique dans les solutions aqueuses de polyélectrolyte: influence de la densité de charge*. PhD thesis, Université Scientifique et Médicale de Grenoble.

Mussel, M., Basser, P. J., and Horkay, F. (2019). Effects of mono-and divalent cations on the structure and thermodynamic properties of polyelectrolyte gels. *Soft matter*, 15(20):4153–4161.

Mussel, M., Basser, P. J., and Horkay, F. (2021). Ion-induced volume transition in gels and its role in biology. *Gels*, 7(1):20.

Muthukumar, M. (2004). Theory of counter-ion condensation on flexible polyelectrolytes: Adsorption mechanism. *The Journal of chemical physics*, 120(19):9343–9350.

Nagasawa, M. and Kagawa, I. (1957). Colligative properties of polyelectrolyte solutions. iv. activity coefficient of sodium ion. *Journal of Polymer Science*, 25(108):61–76.

Nishida, K., Kaji, K., Kanaya, T., and Shibano, T. (2002). Added salt effect on the intermolecular correlation in flexible polyelectrolyte solutions: Small-angle scattering study. *Macromolecules*, 35(10):4084–4089.

Noguchi, H., Gekko, K., and Makino, S. (1973). Interaction of sodium and potassium ions with ionic dextran derivatives in aqueous solution with and without added salt. *Macromolecules*, 6(3):438–442.

Oosawa, F. (1971). *Polyelectrolytes*. Dekker.

O'Shaughnessy, B. and Yang, Q. (2005). Manning-oosawa counterion condensation. *Physical review letters*, 94(4):048302.

Pineda, S. P., Stano, R., Murmiliuk, A., Blanco, P. M., Montes, P., Tosner, Z., Groborz, O., Panek, J., Hruby, M., Stepanek, M., et al. (2024). Charge regulation triggers condensation of short oligopeptides to polyelectrolytes. *JACS Au*, 4(5):1775–1785.

Prabhu, V., Muthukumar, M., Wignall, G. D., and Melnichenko, Y. B. (2003). Polyelectrolyte chain dimensions and concentration fluctuations near phase boundaries. *The Journal of chemical physics*, 119(7):4085–4098.

Ray, D., De, R., and Das, B. (2016). Thermodynamic, transport and frictional properties in semidilute aqueous sodium carboxymethylcellulose solution. *The Journal of Chemical Thermodynamics*, 101:227–235.

Rinaudo, M. (1973). Polyelektrolyteigenschaften von carboxymethylcellulose in wäßriger lösung-einfluß der ladungsdichte1.

Rinaudo, M., B, L., and Milas, M. (1971). Determination of dissociation constant of polyacids by potentiometry. *COMPTES RENDUS HEBDOMADAIRES DES SEANCES DE L ACADEMIE DES SCIENCES SERIE C*, 273(18):1148.

Rinaudo, M. and Loiseleur, B. (1973). Propriétés des solutions aqueuses de polyélectrolytes en présence de sels neutres-ii.—propriétés thermodynamiques. *Journal de Chimie Physique*, 70:1697–1701.

Rinaudo, M. and Milas, M. (1974). Interaction of monovalent and divalent counterions with some carboxylic polysaccharides. *Journal of Polymer Science: Polymer Chemistry Edition*, 12(9):2073–2081.

Rinaudo, M. and Milas, M. (1975). Ionic selectivity of polyelectrolytes in salt free solutions. In *Polyelectrolytes and their Applications*, pages 31–49. Springer.

Rinaudo, M. and Mils, M. (1978). Polyelectroyte behavior of a bacterial polysaccharide from xanthomonas campestris: Comparison with carboxymethylcellulose. *Biopolymers: Original Research on Biomolecules*, 17(11):2663–2678.

Robinson, R. A. and Stokes, R. H. (2002). *Electrolyte solutions*. Courier Corporation.

Różańska, S., Verbeke, K., Różański, J., Clasen, C., and Wagner, P. (2019). Capillary breakup extensional rheometry of sodium carboxymethylcellulose solutions in water and propylene glycol/water mixtures. *Journal of Polymer Science Part B: Polymer Physics*, 57(22):1537–1547.

Salamon, K., Aumiler, D., Pabst, G., and Vuletic, T. (2013). Probing the mesh formed by the semirigid polyelectrolytes. *Macromolecules*, 46(3):1107–1118.

Satake, I., Fukuda, M., Ohta, T., Nakamura, K., Fujita, N., Yamauchi, A., and Kimizuka, H. (1972). Interactions of counterions with dextran sulfate in aqueous solutions. *Journal of Polymer Science: Polymer Physics Edition*, 10(12):2343–2354.

Sharratt, W. N., Lopez, C. G., Sarkis, M., Tyagi, G., O'connell, R., Rogers, S. E., and Cabral, J. T. (2021). Ionotropic gelation fronts in sodium carboxymethyl cellulose for hydrogel particle formation. *Gels*, 7(2):44.

Sharratt, W. N., O'Connell, R., Rogers, S. E., Lopez, C. G., and Cabral, J. T. (2020). Conformation and phase behavior of sodium carboxymethyl cellulose in the presence of mono- and divalent salts. *Macromolecules*, 53(4):1451–1463.

Sircar, S., Keener, J. P., and Fogelson, A. L. (2013). The effect of divalent vs. monovalent ions on the swelling of mucin-like polyelectrolyte gels: Governing equations and equilib-

rium analysis. *The Journal of chemical physics*, 138(1).
Slim, A. H., Shi, W. H., Safi Samghabadi, F., Faraone, A., Marciel, A. B., Poling-Skutvik, R., and Conrad, J. C. (2022). Electrostatic repulsion slows relaxations of polyelectrolytes in semidilute solutions. *ACS Macro Letters*, 11(7):854–860.
Smiatek, J. (2020). Theoretical and computational insight into solvent and specific ion effects for polyelectrolytes: The importance of local molecular interactions. *Molecules*, 25(7):1661.
Sommer, S. (2025). Evaluation of carboxymethyl cellulose as an additive for selective protein removal from wine. *Fermentation*, 11(5):273.
Spiteri, M. N. (1997). *Conformation et arrangement des polyelectrolytes en solution semi-diluee. Etude par diffusion des neutrons aux petits angles*. PhD thesis, Paris 11.
Tang, Q. and Rubinstein, M. (2022). Where in the world are condensed counterions? *Soft Matter*, 18(6):1154–1173.
Tasaki, I. (2012). *Physiology and electrochemistry of nerve fibers*. Elsevier.
Tondre, C., Kale, K., and Zana, R. (1978). Density and ultrasonic absorption studies of the interaction between polyions and hydrophobic counterions. *European Polymer Journal*, 14(2):139–143.
Tondre, C. and Zana, R. (1971). Ultrasonic absorption as a probe for the study of site binding of counterions in polyelectrolyte solutions. *The Journal of Physical Chemistry*, 75(21):3367–3372.
Tondre, C. and Zana, R. (1972). Apparent molal volumes of polyelectrolytes in aqueous solutions. *The Journal of Physical Chemistry*, 76(23):3451–3459.
Tondre, C. and Zana, R. (1975). Comments on letter:" dilatometric study of monovalent counter-ion association with polymethacrylate".
Trivedi, H. C. and Patel, R. D. (1986). Studies on carboxymethylcellulose: Conductivity measurements of solutions, 2. *Die Makromolekulare Chemie: Macromolecular Chemistry and Physics*, 187(1):199–210.
Truzzolillo, D., Cametti, C., and Sennato, S. (2009). Dielectric properties of differently flexible polyions: a scaling approach. *Physical Chemistry Chemical Physics*, 11(11):1780–1786.
Verdugo, P. (2005). Polymer gel phase transition in condensation-decondensation of secretory products. *Responsive Gels: Volume Transitions II*, pages 145–156.
Vlachy, N., Jagoda-Cwiklik, B., Vácha, R., Touraud, D., Jungwirth, P., and Kunz, W. (2009). Hofmeister series and specific interactions of charged headgroups with aqueous ions. *Advances in colloid and interface science*, 146(1-2):42–47.
Wagner, P., Różańska, S., Warmbier, E., Frankiewicz, A., and Różański, J. (2023). Rheological properties of sodium carboxymethylcellulose solutions in dihydroxy alcohol/water mixtures. *Materials*, 16(1):418.
Wandrey, C. (1999). Concentration regimes in polyelectrolyte solutions. *Langmuir*, 15(12):4069–4075.
Wandrey, C., Hunkeler, D., Wendler, U., and Jaeger, W. (2000). Counterion activity of highly charged strong polyelectrolytes. *Macromolecules*, 33(19):7136–7143.
Wang, W., Ji, S., and Xia, Q. (2024). Influence of carboxymethyl cellulose on the stability, rheology, and curcumin bioaccessibility of high internal phase pickering emulsions. *Carbohydrate Polymers*, 334:122041.
Wnek, G. E. (2016). Perspective: Do macromolecules play a role in the mechanisms of nerve stimulation and nervous transmission? *Journal of Polymer Science Part B: Polymer Physics*, 54(1):7–14.

Yoshida, M., Nakagawa, D., Hozumi, H., Horikawa, Y., Makino, S., Nakamura, H., and Shikata, T. (2024). A new concept for interpretation of the viscoelastic behavior of aqueous sodium carboxymethyl cellulose systems. *Biomacromolecules*, 25(6):3420–3431.

Zana, R. (1975). Studies of aqueous solutions of polyelectrolytes by means of ultrasonic methods. *Journal of Macromolecular Science—Reviews in Macromolecular Chemistry*, 12(2):165–189.

Zana, R. and Tondre, C. (1975a). Ultrasonic studies of polyion polyelectrolytes solutions. *Chemical and Biological Applications of Relaxation Spectrometry: Proceedings of the NATO Advanced Study Institute Held at the University of Salford, Salford, England, 29 August–12 September, 1974*, 18:333.

Zana, R. and Tondre, C. (1975b). Ultrasonic studies of polyion—counterion interactions in polyelectrolytes solutions. In *Chemical and Biological Applications of Relaxation Spectrometry: Proceedings of the NATO Advanced Study Institute held at the University of Salford, Salford, England, 29 August–12 September, 1974*, pages 333–341. Springer.

Zana, R., Tondre, C., Rinaudo, M., and Milas, M. (1971). Étude ultrasonore de la fixation sur site des ions alcalins sur des carboxymethylcelluloses de densité de charge variable. *Journal de Chimie Physique*, 68:1258–1266.

Zhang, M., Xu, T., Zhao, Q., Liu, K., Liang, D., and Si, C. (2024). Cellulose-based materials for carbon capture and conversion. *Carbon Capture Science & Technology*, 10:100157.

Zhang, W., Liu, Y., Xuan, Y., and Zhang, S. (2022). Synthesis and applications of carboxymethyl cellulose hydrogels. *Gels*, 8(9):529.

Zhang, Y., Douglas, J. F., Ermi, B. D., and Amis, E. J. (2001). Influence of counterion valency on the scattering properties of highly charged polyelectrolyte solutions. *The Journal of Chemical Physics*, 114(7):3299–3313.

Zhou, C., Chen, K., Zheng, K., Yang, J., and Zhao, J. (2024). Counterions redistribution of a polyelectrolyte induced by shear flow. *Macromolecules*, 57(12):5739–5746.

Statements and Declarations

This work was supported by DFG (grant number GO 3250/2-1) and JSPS KAKENHI (Grant numbers JP24K01236 and JP20KK0325).

The authors have no relevant financial or non-financial interests to disclose.